© by PSP Volume 28 (11A) – No. 2019, pages 8649-8658 Fresenius Environmental Bull

MECHANISM OF CAPSEBON NANOPARTICLES INDUCED OXIDATIVE STRESS AND APOPTOSIS IN CACO-2 CELLS

Mohammed S Aleissa[1], Daoud Ali[2,*], Saud Alarifi[2], Saad Alkahtani[2]

[1] Department of Biology, Science College, Al-Imam Muhammad Ibn Saud, Islamic University, Riyadh, Saudi Arabia.
[2]Department of Zoology, College of Science, King Saud University, Riyadh, Saudi Arabia

ABSTRACT

Capsebon (CdS) nanoparticles are extensively used in excipients, drugs and paints, plastics, textiles, ceramic and glass industry. The high exposure to capsebon nanoparticles causes adverse effect on skin, eyes, respiratory track and kidney. The toxicity profile of capsebon nanoparticles on human colon cancer (Caco-2) cells is not finally understood. Hence, in this study capsebon nanoparticles were characterized were characterized by UV-visible spectrophotometer, dynamic light scattering and transmission electron microscope. The cell toxicity of capsebon nanoparticles was observed in Caco-2 cells by using NRU and MTT tests. The percentage of cell death was increased as the dose and time of capsebon nanoparticles exposure was increased. The hike in the production of reactive oxygen species (ROS) in Caco-2 cells due to capsebon nanoparticles was checked by applying fluorescent dye DCFDA and production of ROS was time and dose dependent. The toxicity of capsebon nanoparticles in Caco-2 cells was correlated with the generation of ROS, compromisation of mitochondrial trans membrane potential (MTP) and nucleic acid damage. Thus the current observation was confirmed that mitochondria play an important role in genotoxicity and cytotoxicity induced capsebon nanoparticles in Caco-2 cells. Also, we have examined the oxidative stress biomarkers lipid peroxide (LPO), and glutathione (GSH) and LPO was increased and GSH was decreased in Caco-2 cells. In this experiment, we noticed that capsebon nanoparticles are more dangerous at higher dose and increased time. This work deals the dose and dependent cell toxicity and apoptosis in Caco-2 cells

KEYWORDS:
Capsebon nanoparticles; Caco-2 cells; Oxidative stress; Cytotoxicity

INTRODUCTION

The application of nanotechnology in drugs and health related industry is rapidly growing and it was more than 1.2 trillion USD in 2017. In the current scenario the engineered nanoparticles are extensively used in per day life in the form of cosmetics, drugs, food packaging, therapeutics, biosensors, and with these, unprecedented avenues for exposure of nanoparticles (NPs) to the environment and living beings are increasing [1]. The growing application of nano-materials makes it imperative to find out the hazardous effect of nanoparticles based substances; as due to their unique physio chemical characteristic such as shape, size, crystal structure, agglomeration, surface charge, surface area, solubility in conveying toxic manifestations. Keeping in mind of these facts capsebon nanoparticles is used for to assess its toxicity on human colon cancer (Caco-2) cell lines.

Cadmium-loaded nanomaterials are extensively applied in electronic and biological applications [2]. Some researchers reported the toxic effects of cadmium compound on animal and human health. Gastrointestinal ingestion of Cd through food or drinking water is the major route of intake for this metal in non smoking and non-occupationally exposed populations [3]. Cigarette smoke is the highest source of Cd exposure in all populations [4]. Each cigarette could contain up to 6.67 µg Cd, and 40-60% of it generally passes through the pulmonary epithelium into systemic circulation [4].

This is supposed that nanoparticles may mess up and damage cell function through a different type of mechanism [5]. The nanoparticle has some ions or toxic materials which indirectly or directly affect the living cells via production of reactive oxygen species (ROS). Really, It is reported that cell toxicity occurred due to xenobiotic materials, nanoparticles due to ROS generation [6, 7]. Also, an independent component of nanoparticles can induce cellular damage due to their ability to adhere to or to pass through cell membranes [8].

Capsebon nanoparticles are a known carcinogen and are associated with an elevated risk of developing lung cancer.The high level of reactive oxygen species (ROS) generation induced DNA strand breakage, damaging cellular macromolecules (proteins, fat, carbohydrate) and apoptosis. The mechanism of action by which capsebon nanoparticles exerts its toxic effects remains unclear. Thus, we aimed to evaluate the cytotoxicity and the genotoxicity induced by capsebon nanoparticles on

human colon carcinoma cells (Caco-2), being one of the target cells exposed to these nanoparticles following the ingestion of contaminated products.

MATERIALS AND METHODS

Chemical and reagents. Capsebon nanoparticles (APS<10 nm particle size) was purchased from US Research Nanomaterials, Inc. MTT (1-(4,5-Dimethylthiazol-2-yl)-3,5-diphenylformazan, Thiazolyl blue formazan), neutral red dye, 5, 5-dithiobis-(2-nitrobenzoic acid) (DTNB), 2, 7-dichlorofluorescein diacetate (H2-DCFH-DA), dimethyl sulfoxide (DMSO), annexin V FITC and propidium iodide (PI) were obtained from Sigma-Aldrich. Dulbecco's modified Eagle's medium (DMEM), fetal bovine serum (FBS) and antibiotics were purchased from Gibco, USA. All other chemicals were purchased from local suppliers.

Cell line and culture. Human colon cancer (Caco-2) cells were brought from Research Center King Faisal Specialty Hospital Riyadh, Saudi Arabia. Caco-2 cells were cultured in DMEM culture medium added with FBS (10%) and 100 U/ml antibiotics at CO_2 (5%) incubator at 37°C. At near about 75 % confluence, cells were sub cultured into 96 well plates, 6 well plates and 25 cm^2 flasks according to design experiments.

Treatments of capsebon nanoparticles. Caco-2 cells were cultured for one day before exposure to capsebon nanoparticles. The stock suspension of capsebon nanoparticles was made by adding 1 mg nanoparticles in to one ml culture medium and diluted according to the experimental dosages (1-45 µg/ml). The nanoparticle was dispersed in suspension by sonication at 40 KHz for 15 min at room temperature prior to treatment. The control cells were not exposed to capsebon nanoparticles.

Characterization of capsebon nanoparticles. Transmission Electron Microscopy (TEM). The stock solution of capsebon nanoparticles (1 mg/ml) was made in double distilled water. The carbon coated copper grid was dipped in suspension of the highest dose of capsebon nanoparticles (45 µg/ml) solution and it was dried for 24 h. After dried the grid, the photomicrograph of capsebon nanoparticles was captured by using transmission electron microscope (TEM) (JEOL Inc., Tokyo, Japan) at 120 kV. We have counted 10 areas of TEM grid.

Dynamic light scattering (DLS0). The size and zeta potential of nanoparticles in aqueous solution were examined by using dynamic light scattering (DLS, Nano-Zeta Sizer-HT, Malvern, UK) as described by Alarifi et al. [9]. The capsebon nanoparticles powder was suspended (45 µg/ml) in double distilled water and culture media. The nanoparticle suspension was sonicated at 40 W for 10 minutes by sonicator.

Morphological analysis of cells. The effect of capsebon nanoparticles on the morphology of Caco-2 cells was seen under inverted phase contrast microscope (Nikon Eclipse Ti-S Japan). The cells were exposed to different concentration of capsebon nanoparticles (0, 1, 3, 15, 45 µg/ml) for 48 hours.

The morphology of cells was observed by using inverted phase contrast microscope (Nikon Eclipse Ti-S Japan).

MTT assay. The cytotoxic potential of capsebon nanoparticles in Caco-2 cells was determined by MTT assay as described by Alarifi et al. [9]. In short, 1×10^4 cells/ well were seeded in a culture plate (96-well) and exposed to capsebon nanoparticles (0, 1, 3, 15, 45 µg/ml) for 48 h. After exposure, the culture media was removed from 96 well plates and 100 µL MTT solution per well and incubated at 37°C for a minimum of 3 h. After incubation again the culture plates wre washed with chill PBS and dissolve the formazon crystal by dissolving in dimethylsulphoxide and the optical density was recorded as relative colorimetric changes measured at 570 nm using a micro plate reader (Synergy-HT; BioTek, Winooski, VT, USA).

NRU test. The effect of capsebon nanoparticles (0, 1, 3, 15, 45 µg/ml) on Caco-2 cells for 48 h was determined by neutral red uptake test according method of Borenfreund and Puerner [10]. Later the exposures of nanoparticles, the cells were washed with chilled saline buffer and added neutral red dye (100 µl) with DMEM for 4 hour and after incubation the cells were washed with fixative and simultaneously dye extractor solution. The optical density was taken at 540 nm [10].

Generation of reactive oxygen species (ROS). The generation of ROS in Caco-2 cells after exposure to capsebon nanoparticles (0, 1, 3, 15, 45 µg/ml) were examined according method of Alarifi et al., [9]. We have cultured the cells (2×10^4 cells/well) in 96-well black plates for 20 h and then treated with nanoparticles for 24 and 48 h. After exposure cells were incubated with H2DCF-DA for 30 min. After incubation, the fluorescence of dichlorofluorescin was evaluated by using fluorescence micro-plate reader (Spectra MAX Gemini EM, Molecular Devices) at 480-nm (excitation wavelength) and 530 nm (emission wavelength).

For qualitative analysis of ROS generation in Caco-2 cells due to nanoparticles, we have set simultaneously another experiment in a six-well transparent plate ($1x10^3$ cells/well) and intracellular ROS

generation was seen by using a fluorescent microscope (Olympus CKX41; Olympus: Center Valley, Pennsylvania, USA), with images taken at 10 X magnification.

Cell lysate. The nanoparticle (0, 1, 3, 15, 45 µg/ml) exposed Caco-2 cells and non-exposed cells were washed with cold phosphate buffer saline and collected in an eppendrof tube through scraping. The lysis buffer was added in collected cells and centrifuged at 13000 rpm for 10 min at 4ºC and the supernatant (cell lysate) was maintained on ice for further tests for reduced glutathione (GSH) and lipid peroxide (LPO).

The amount of protein in cell lysate was determined by the Bradford method [11] using bovine serum albumin as the standard.

GSH test. The content of GSH was evaluated by according Ellman's method [12]. Cell lysate 100 µl was added TCA (5%, TCA 900 µl) and centrifuged at 3000 g for 10 min at 4 °C. Again 500 µl supernatant was added with DTNB (0.01%, 1.5 ml) and OD of the mixture was observed at 412 nm. The quantity of glutathione was represented in (%) percentage as compared with the control.

LPO test. Lipid peroxide (LPO) was determined according Ohkawa et al. [13]. Shortly, cell lysate (100 µl) was mixed with 1.9 ml sodium phosphate buffer (0.1 M, pH 7.4) and incubated for 60 min 37°C. After incubation 5% TCA was added and centrifuged at 3000 g for 10 min at room temperature) to obtain a supernatant. The supernatant was mixed with 1 ml TBA (1%) and put in a water bath at 100 °C for 30 min. The optical density of the cooled mixture was examined at 532 nm and was converted to MDA and expressed in terms of percentage as compared with the control.

Mitochondrial transmembrane potential (MTP). Mitochondrial transmembrane potential (MTP) was observed by using JC-1 fluorescent staining. Capsebon nanoparticles (1, 3, 15, 45 µg/ml) exposed to Caco-2 cells for 24 and 48 h. After exposure to fixed time the cells were washed and incubated with JC-1 (5 µM, Cayman chemical) for 30 min at 37°C.Then the plate was washed and images were taken by fluorescence microscope [7].

A parallel experiment was carried out to determine the J-aggregate and J-monomer ratios [7]. Both cell lines were seeded in a black well-plate (96-well) and incubated with different concentrations of Capsebon nanoparticles (1, 3, 15, 45 µg/ml) for 24 and 48 h. After incubation, the fluorescence of the J-aggregates and J-monomers were evaluated by using a fluorescence microplate reader (Spectra MAX Gemini EM, Molecular Devices) at 530/590 nm (excitation wavelength/emission wavelength) for the J-aggregates and 480/528 nm (excitation wavelength/emission wavelength) for the J-monomers.

Assessment of chromosome condensation and caspase-3 activity. The chromatin condensation in Caco-2 cells after exposure to nanoparticles was visualized by DAPI staining. The condensed chromatin body in exposed cells was observed according to Toné et al. method [14].

The alteration of caspase-3 level was seen Caco-2 cells after exposure to nanoparticles by using Cayman Chemical colourimetric assay kits.

Alkaline single cell gel electrophoresis. DNA damage in Caco-2 cells was observed by comet assay according Ali et al.[15]. The cells (50000 cells per well) in six well plate was cultured and exposed to capsebon nanoparticles (0, 1, 3, 15 µg/ml) for 24 and 48 h. After exposure the cells were trypsinized and centrifuged at 1200 rpm for 5 mn and suspended in cold culture medium. Twenty thousand cells (15 µl) were mixed with low melting point agarose (85 µl, 0.5%) and embedded in precoated agaorse slide. After solidification of slide, it was immersed in lysis buffer for 24 h and the next day it was immersed in alkaline electrophoresis buffer for 20 mn for DNA strand unwinding and electrophoresis was done at 300 mA, 16 mV for 30 mn. After electrophoresis the slide was washed through neutralizing solution and stained with ethidium bromide. The cell image of 50 random cells (25 from each replicate slide) was analyzed for each experiment. Single strand breakage was determined as % tail DNA and olive tail moment (OTM) by using Kamet software

Statistical analysis. The significant value of the present data was analyzed by using one-way analysis of variance (ANOVA) and the significant value was fixed at (*$p<0.05$, **$p<0.01$). Data were expressed as the average value of triplicate independent experiments.

RESULTS

Characterization of capsebon nanoparticles. Size, surface area, structure and morphology of nanoparticles were examined by high resolution transmission electron microscope (HR-TEM) and dynamic light scattering (DLS) methods. We have counted 100 separate nanoparticles for size determination.

The average size of 100 capsebon nanoparticles was 15.30±2.7 nm. Fig. 1A showed the TEM image of capsebon nanoparticles. Average size, frequency (%) of capsebon nanoparticles was presented in Fig. 1B. The hydrodynamic size of capsebon nanoparticles was 176 nm and zeta -potential -13.4 mV.

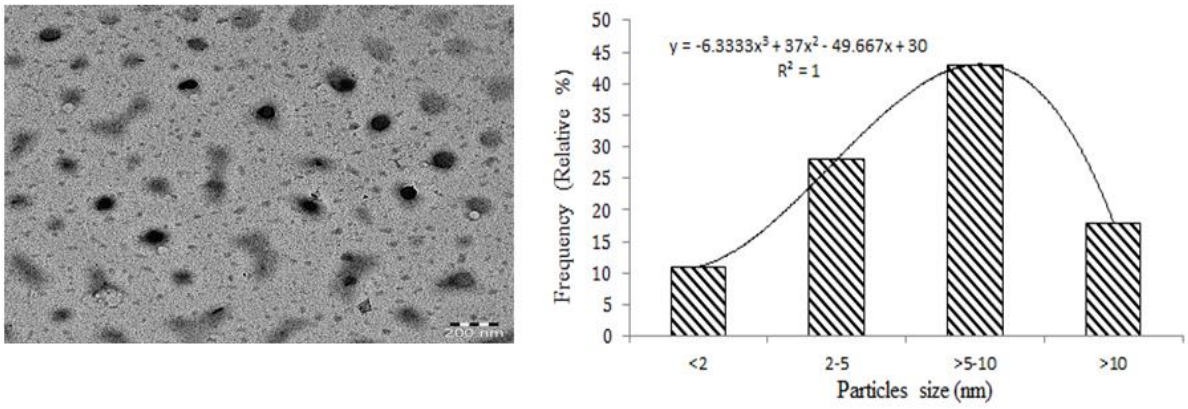

(A) (B)

FIGURE 1
(A) TEM image of capsebone nanoparticles (B) Frequency (%) of capsebone nanoparticles size distribution.

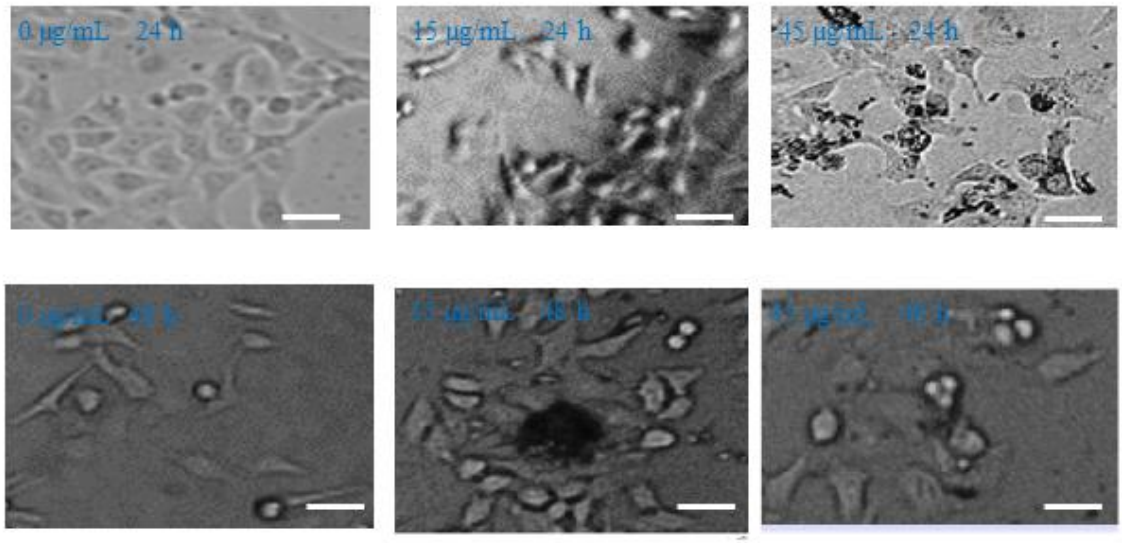

FIGURE 2
Alteration in morphological Caco-2 cells exposed to different concentrations of capsebone nanoparticles for 24 h and 48 h.Scale bar is 200 µm.

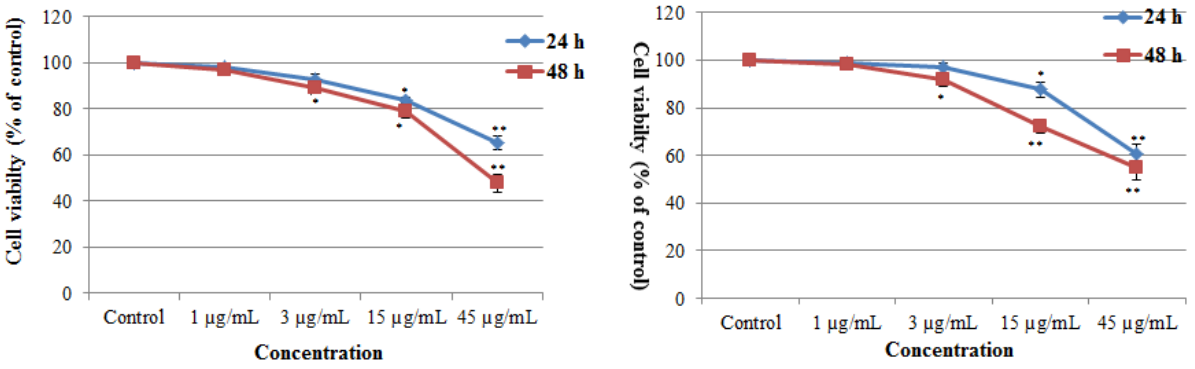

(A) (B)

FIGURE 3
Cytotoxicity of capsebone nanoparticles in Caco-2 cells for 24 and 48 h, as determined by (A).MTT (B). NRU tests.Each value represents the mean ±SE of three experiments. n=3, *p <0.05, **p <0.01 vs. control.

Morphology of Caco-2 cells. The alteration in morphology of Caco-2 cells was examined by using upright phase contrast microscope. After exposure to capsebon nanoparticles the morphology of cells was changed into round, ruptured cell membrane and detached from a culture flask (Fig. 2). More cells are becoming round shape and ruptured at higher concentration of capsebon nanoparticles (45 µg/ml) (Fig. 2). On the other hand the cells were not affected at lower dose of nanoparticles below (3 µg/ml) (Fig. 2).

Cytotoxicity. The cell toxicity of capsebon nanoparticles was examined for 24 and 48 h and it was done by observing the mitochondrial activity and lysosome activity by using MTT and NRU assays, respectively. The present data of MTT test demonstrated that the viability of cells were 98.06 %, 92.9 %, 83.6 % and 65.5 % for 24 h, and 97 %, 89% , 78.95% and 47.62% (Fig. 3A). Capsebon nanoparticles induced cytotoxicity in a concentration and time-dependent manner. The results of NRU assay were accorded with the MTT assay (Fig. 3B).

Oxidative Stress. After exposure to capsebon nanoparticles for 24 and 48 h, the reactive oxygen species were generated in Caco-2 cells. The Caco-2 cells showed high intensity of dichlorofluorescin as green fluorescence (as a marker of intracellular ROS generation) as compared to control when exposed to capsebon nanoparticles (45 µg/ml) (Fig. 4A).

The intracellular ROS generation was dose and time dependent (Fig. 4B). The more generation of ROS was measured in 45 µg/ml of nanoparticles exposed Caco-2 cells and it increased 200 % than control (100%) for 48 h.

Lobo et al. [16] suggested that antioxidants, free radicals or reactive oxygen species (ROS) can cause direct impairment to carbohydrate, proteins and lipids. The ratio of MDA, which is a final product of LPO, was significantly hiked (Fig. 5A) but on the other hand GSH level was reduced (Fig. 5B) as a concentration and time-dependent manner in capsebon nanoparticles treated cells.

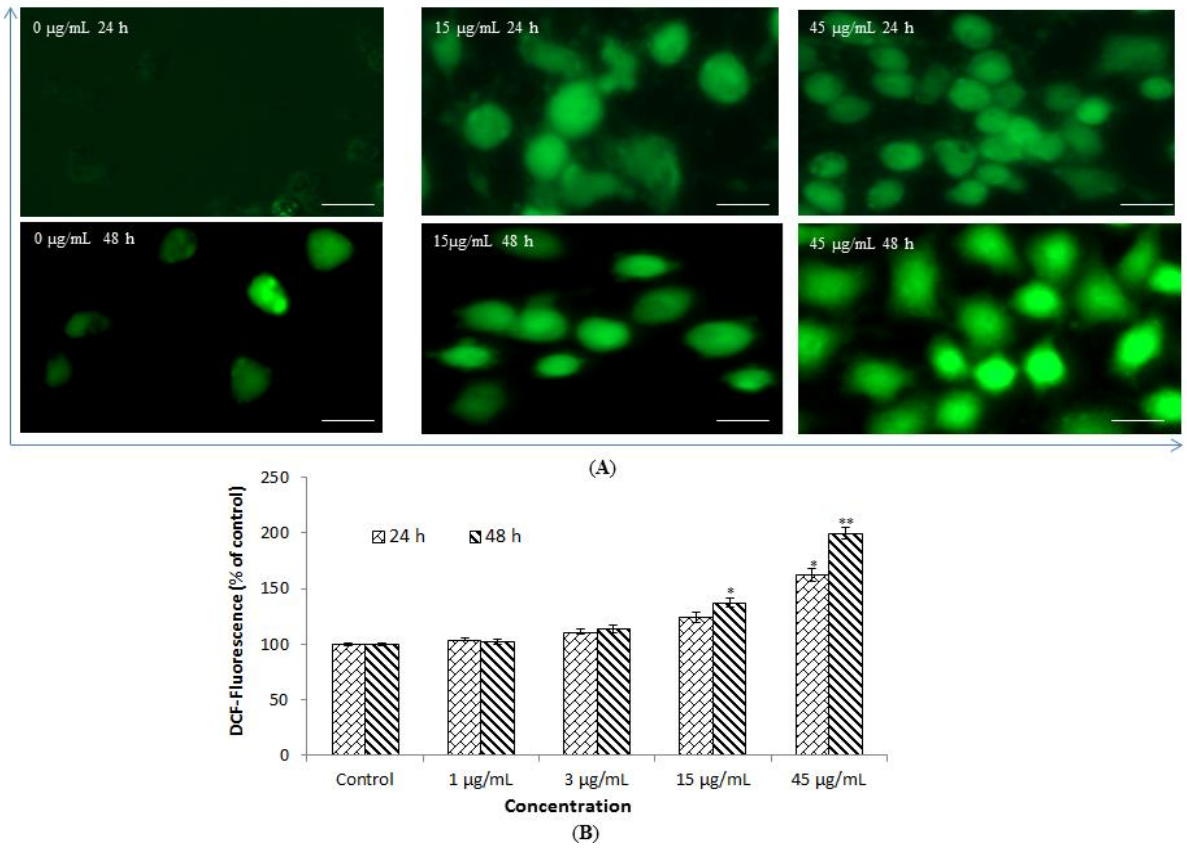

FIGURE 4

Production of ROS after exposure to capsebone nanoparticles (A) Fluorescence images of Caco-2 cells treated with 15µg/ml and 45 µg/ml of casebone nanoparticles for 24 h and 48 h and stained with DCFDA (B) % ROS production due to capsebone nanoparticles in Caco-2 cells.Each value represents the mean ±SE of three experiments. *p <0.05, **p <0.01 vs. control.
Scale bar is 200 µm.

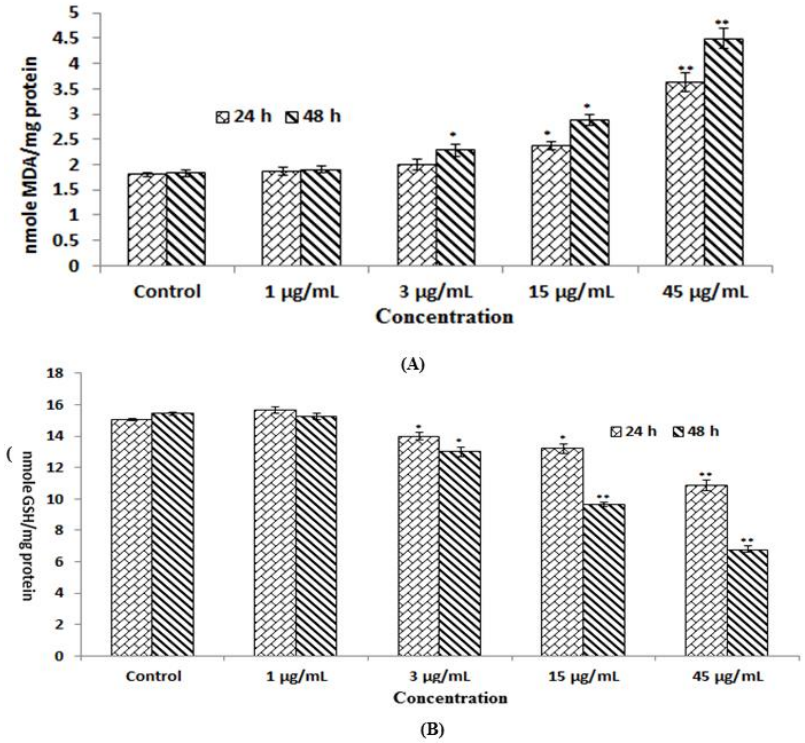

FIGURE 5

(A). Levels of LPO (B) GSH in Caco-2 cells due to capsebone nanoparticles treatment for 24 h and 48 h. Each value represents the mean ±SE of three experiments. *p <0.05, **p <0.01 vs. control.

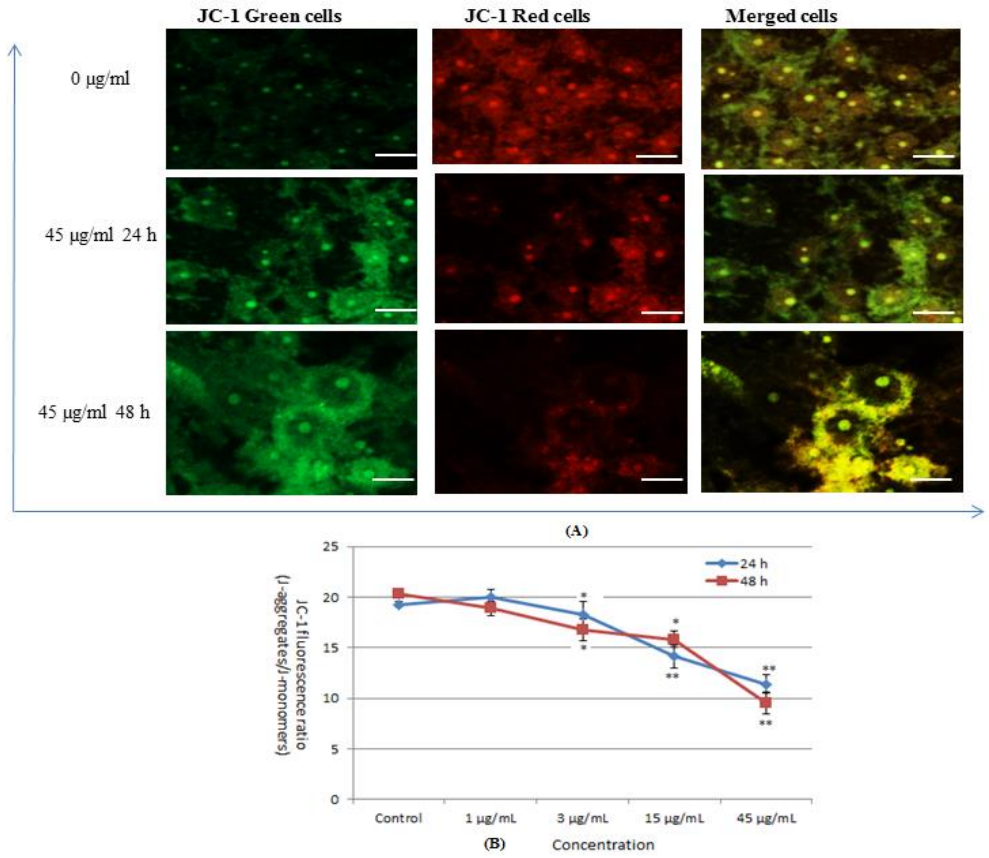

FIGURE 6

Mitochondrial transmembrane potential (MTP) in Caco-2 cells due to capsebone nanoparticles (A) Photomicrograph of JC-1 fluorescence intensity (B) JC-1 fluoresencence rate as marker of MTP los. Each value represents the mean ±SE of three experiments. *p <0.05, **p <0.01 vs. control. Scale bar is 200 µm.

MTP. After exposure of capsebon nanoparticles to Caco-2 cells, the compromised MTP was determined by JC-1 fluorescent dye staining method on the principle of development of J-aggregate and J monomer. Hirsch et al. [17] has been reported that mitochondrial permeability of apoptotic and necrotic cell was compromised due to oxidative stress. The strong MTP was found in control (0 µg/mL) Caco-2 cell as JC-1 dye penetrates to cells and produced J aggregates, with deep red fluorescence (Fig. 6A). MTP was compromised in the exposed Caco-2 cell as a result J monomer with high intensity of green fluorescence was formed (Fig. 6A). The ratio of J-aggregates and J-monomers were decreased in Caco-2 cells at higher concentration of nanoparticles exposure for 24 and 48 h (Fig. 6B).

Apoptosis. In this experiment we have examined the apoptotic effect of capsebon nanoparticles in Caco-2 cells by using different parameters such as chromosome condensation and caspase- 3 activity in apoptotic and necrotic cell. Control cells showed intact nucleus with blue fluorescence, but apoptotic cells have fragmented chromatin with high blue intensity (Fig. 7A).

The activity of caspase-3 (trademark of apoptosis) is increased in capsebon nanoparticles treated cells as compared to control (Fig. 7B). The activity of the caspase-3 enzyme was significantly increased dose and time dependent manner (Fig. 7B).

DNA damage. The effect of capsebon nanoparticles on nuclear materials such as DNA of Caco-2 cells was seen by using alkaline single cell gel test. The cells showed more DNA damage as the capsebon nanoparticles concentration and duration of exposure was increased as compared to control (Fig. 8C).

In capsebon nanoparticles exposed Caco-2 cells the % tail DNA was found higher than to control (Fig. 8A). Also, the high olive tail moment (4.52 AU) was seen in capsebon nanoparticles cells than control (1.08 AU) for 48 h at 45µg/ml (Fig. 8B).

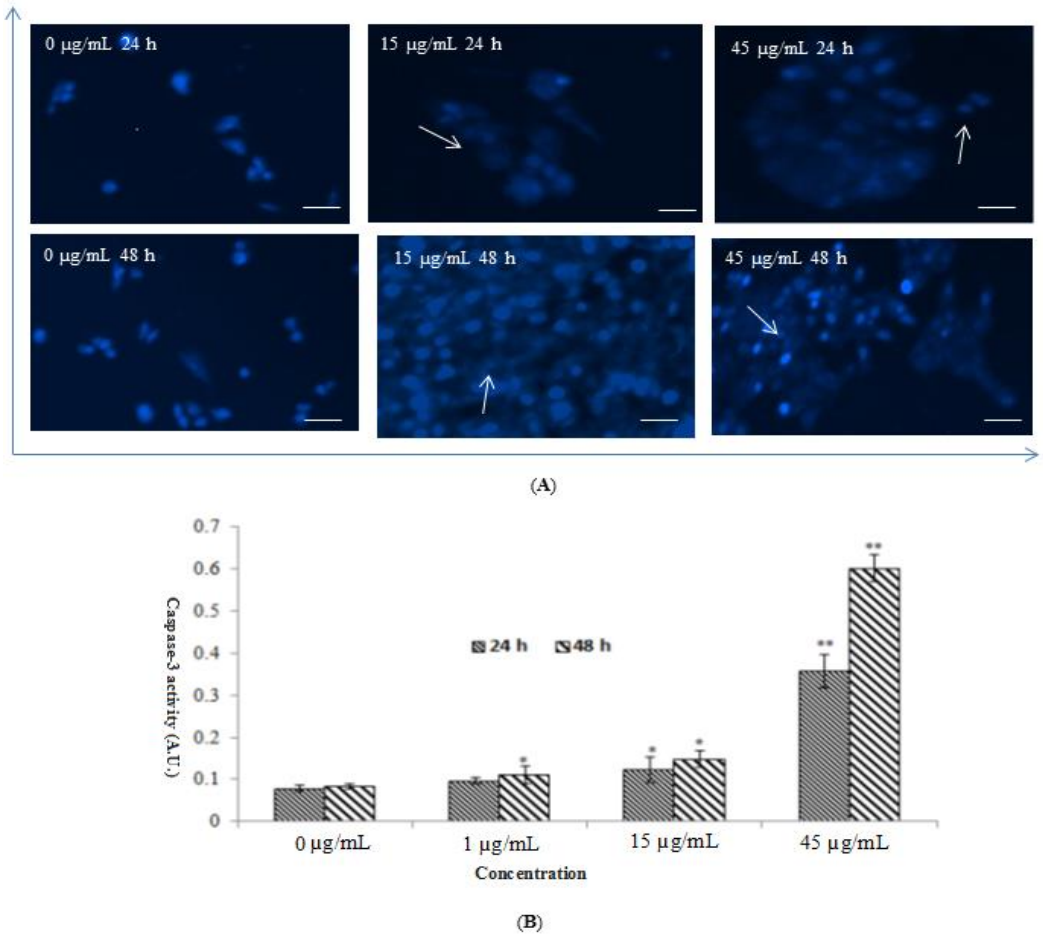

FIGURE 7

(A). Chromosomal condensation and (B) Induction of caspase-3 activity in Caco-2 cells after exposure to capsebone for 24 h and 48 h. Each value represents the mean ±SE of three experiments. *p <0.05, **p <0.01 vs. control. Arrow indicates fragmented chromosome. Scale bar is 200 µm.

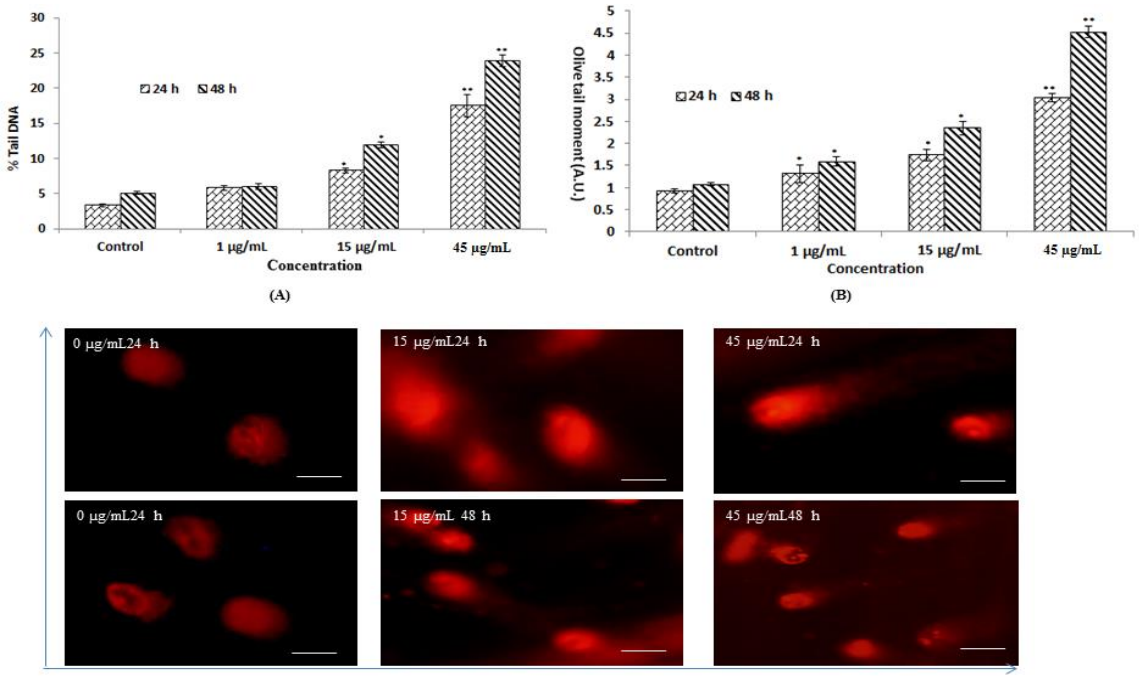

FIGURE 8
DNA damage in Caco-2 cells ue to capsebone nanoparticles (A) Tail DNA (%) (B) Olive tail moment (C) DNA damage photomicrograph of Caco-2 cells due to casebone nanoparticles. Each value represents the mean ±SE of three experiments. *p <0.05, **p <0.01 vs. control. Scale bar is 50 µm.

DISCUSSION

Due to unique physical chemical properties of nano-size particles resulted more toxicity when compared to macro size particles. Hence, in this study we have carried out with aim to find out the apoptotic and genotoxic efficacy of capsebon nanoparticles on Caco-2 cells. The used capsebon nanoparticles as reported by suppliers were 10 nm however, the determined the nanoparticles size by TEM and DLS were more than the original size.

In comparison to measurements in the dry phase (by TEM) the mean particle sizes and size distributions of particles (measured by DLS) were enhanced when measured in aqueous media. Due to high specific surface area and high surface energy level, nanoparticles have the propensity to aggregate together to form micro-size particles that are more stable in the environment [18, 19]. So, to protect the formation of agglomeration, a colloidal suspension of nanoparticles, the suspension of capsebon nanoparticles was prepared freshly and sonicated prior to the experiment.

The size and structure of capsebon nanoparticles have an important effect on their work. The same size and shape is basic properties of nanoparticles that are important for their biological activities. Mostly capsebon nanoparticles have round-shape structure. Nanoparticles caused harmful effect due to surface chemistry, size and shape [20].

In the current experiment we have evaluated the toxic potential of capsebon nanoparticles in Caco-2 cells by using MTT, and NRU tests. The intracellular produced free radicals affected on cell organelles and cellular substances such as carbohydrate, fats, proteins and DNA molecules [21]. Capsebon nanoparticles increased the caspase-3 activity and number chromatin condensed Caco-2 cells. Also the quantity of fragmented DNA was increased in exposed cells as compared to control cells. The production of intracellular ROS and changed redox status are normal physiochemical phases in Caco-2 cells. ROS may be interacting with fatty acids of plasma membrane and produces peroxidation of lipid. The final bio product of lipid peroxidation, such as malondialdehyde has been contemplating to be a second messenger of oxidative stress [22].

On the other hand surplus intracellular ROS production was occurring due to capsebon nanoparticles as a result oxidative damage and apoptosis occurred [23]. Generation of ROS, declination of GSH, lipid peroxides and DNA damage due to capsebon nanoparticles in cells leading to damage cellular component of cells. Some researchers are documented that cadmium sulfide nanoparticles induced toxicity and apoptosis in human cell lines and chicken embryos [24]. To find out the probable cause of nanoparticle induced cell death, we examined the alteration of different biomarkers involved in apoptosis. Susin et al. [25] suggested that mitochondria play an important role in apoptosis and the compromise of mitochondrial integrity may be prevented by various biomarkers of apoptosis. Oxidative stress leads to activation of caspase enzymes via involvement of cytochrome-c in the

inter membrane space into cytoplasm [26].

In the present study capsebon nanoparticles declined the mitochondrial membrane potential. In this study we found the compromisation of mitochondrial membrane potential due to capsebon nanoparticles as a result of apoptosis occurred. Our results showed caspase-3 activity was increased time and dose dependent manner. Mitochondria play significant role in metal toxicity through inducing intracellular ROS generation [27]. This puts forward that capsebon nanoparticles inductees the intrinsic pathway of apoptosis, which is mediated by increasing caspase-3 activity and loss of mitochondria trans membrane potential.

CONCLUSIONS

On the basis of above finding we conclude that capsebon nanoparticles produced intracellular ROS and compromising the level of glutathione and provoked to damage the nuclear molecule and cell organelles of Caco-2 cells. Capsebon nanoparticles compromise to apoptosis via mitochondrial and caspase-3 dependent on Caco-2 cells.

Declaration of conflicting interests. None

ACKNOWLEDGEMENTS

The researchers acknowledge the Deanship of Scientific Research at Al Imam Mohammad Ibn Saud Islamic University, Saudi Arabia, for funding this project under the grant no. 731228.

REFERENCES

[1] Seshan, K. (2002) Handbook of Thin-Film Deposition Processes and Techniques-Principles, Methods, Equipment and Applications.Noyes, Minn, USA: William Andrew Publishing;.

[2] Bowers, M.J., McBride, J.R., Rosenthal, S.J. (2005). White light emission from magic-sized cadmium selenide nanocrystals. J. Am. Chem. Soc. 127, 15378.

[3] Godt, J., Scheidig, F., Grosse-Siestrup, C., Esche, V., Brandenburg, P. et al. (2006) The toxicity of cadmium and resulting hazards for human health. J Occup Med Toxicol. 10, 1-22.

[4] Arroyo, V.S., Flores, K.M., Ortiz, L.B., Gómez-Quiroz, L.E., Gutiérrez, R.M.C. (2012) Liver and Cadmium Toxicity. J Drug Metab Toxicol. S5

[5] Huang, Y.W., Cambre, M., Lee, H.J. (2017) The toxicity of nanoparticles depends on multiple molecular and physicochemical mechanisms. Int. J. Mol. Sci. 18, 2702.

[6] Markovic, Z., Trajkovic, V. (2008) Biomedical potential of the reactive oxygen species generation and quenching by fullerenes (C60). Biomaterials. 29(26), 3561-73.

[7] Alarifi, S., Ali, H., Alkahtani, S., Aleissa, M.S.(2017) Regulation of apoptosis through bcl-2/bax proteins expression and DNA damage by nano-sized gadolinium oxide. Int J Nanomedicine. 12, 4541-4551.

[8] Verma, A., Uzun, O., Hu, Y., Hu, Y., Han, H.S., Watson, N., Chen, S., Irvine, D.J., Stellacci, F. (2008) Surface-structure-regulated cell-membrane penetration by monolayer-protected nanoparticles.Nat Mater. 7(7),588-95.

[9] Alarifi, S., Ali, D., Alkahtani, S. (2015) Nanoalumina induces apoptosis by impairing antioxidant enzyme systems in human hepatocarcinoma cells," International Journal of Nanomedicine. 10 (1), 3751-3760.

[10] Borenfreund, E., Puerner, J.A. (1985) Toxicity determined in vitro by morphological alterations and neutral red absorption, Toxicology Letters. 24, 2-3,119-124.

[11] Bradford, M.M. (1976) A rapid and sensitive method for the quantitation of microgram quantities of protein utilizing the principle of protein dye binding. Anal. Biochem. 72, 248-254.

[12] Ellman, G.L. (1959) Tissue sulfhydryl groups. Arch. Biochem. Biophys. 82, 70-77.

[13] Ohkawa, H., Onishi, N., Yagi, K. (1979) Assay for lipid peroxidation in animal tissue by thiobarbituric acid reaction Anal. Biochem. 95, 351-358.

[14] Toné, S., Sugimoto, K., Tanda, K., Suda, T., Uehira, K., Kanouchi, H., Samejima, K., Minatogawa, Y., Earnshaw, W.C. (2007) Three distinct stages of apoptotic nuclear condensation revealed by time-lapse imaging, biochemical and electron microscopy analysis of cell-free apoptosis. Exp Cell Res. 313(16), 3635-3644.

[15] Ali, D., Nagpure, N.S., Kumar, S., Kumar, R., Kushwaha, B. (2008) Genotoxicity assessment of acute exposure of chlorpyrifos to freshwater fish Channa punctatus (Bloch) using micronucleus assay and alkaline single-cell gel electrophoresis. Chemosphere. 71,1823-1831.

[16] Lobo, V, Patil, A., Phatak, A., Chandra, N. (2010) Free radicals, antioxidants and functional foods: Impact on human health. Pharmacognosy Reviews. 4(8),118-126.

[17] Hirsch, T., Susin, S., Marzo, I. et al. (1998) Mitochondrial permeability transition in apoptosis and necrosis**.** Cell Biol Toxicol. 14, 141-145.

[18] He, Y.T., Wan, J., Tokunaga, T. (2008) Kinetic stability of hematite nanoparticles: the effect of particle sizes, Journal of Nanoparticle Research. 10 (2), 321-332.

[19] Petosa, A.R., Jaisi, D.P., Quevedo, I.R., Elimelech, M., Tufenkji, N.(2010) Aggregation and deposition of engineered nanomaterials in aquatic environments: role of physicochemical interactions, Environmental Science and Technology. 44(17), 6532-6549.
[20] Sharma, D., Kanchi, S., Bisetty, K. (2015) Biogenic synthesis of nanoparticles. A review. Arabian Journal of Chemistry.
[21] Gaetke, L.M., Chow, C.K. (2003) Copper toxicity, oxidative stress, and antioxidant nutrients Author links open overlay panel. Toxicology. 189(1-2), 147-163.
[22] Barrera, G. (2012) Oxidative Stress and Lipid Peroxidation Products in Cancer Progression and Therapy. ISRN Oncology, Volume 2012, Article ID 137289, 21 pages.
[23] Beckhauser, T.F., Oliveira, J. F., Pasquale, R. De. (2016) Reactive Oxygen Species: Physiological and Physiopathological Effects on Synaptic Plasticity Supplementary Issue: Brain Plasticity and Repair. Journal of Experimental Neuroscience. 10(S1), 23-48.
[24] Rodríguez-Fragoso, P., Reyes-Esparza, J., León-Buitimea, A., Rodríguez-Fragoso, L. (2012) Synthesis, characterization and toxicological evaluation of maltodextrin capped cadmium sulfide nanoparticles in human cell lines and chicken embryos. Journal of Nanobiotechnology. 10, 47
[25] Susin, S.A., Zamzami, N., Kroemer, G. (1998) Mitochondria as regulators of apoptosis: doubt no more. Biochimica et Biophysica Acta (BBA) - Bioenergetics. 1366 (1-2); 151-165.
[26] Yuan, J., Murrell, G.A.C., Trickett, A., Wang, M.X. (2003) Involvement of cytochrome *c* release and caspase-3 activation in the oxidative stress-induced apoptosis in human tendon fibroblasts. Biochimica et Biophysica Acta (BBA) - Molecular Cell Research. 1641 (1), 35-41.
[27] Keunen, E., Remans, T., Bohler, S., Vangronsveld, J. (2011) Cuypers A. Metal-Induced Oxidative Stress and Plant Mitochondria, Int. J. Mol. Sci. 12, 6894-6918.

Received: **14.04.2019**
Accepted: **17.06.2019**

CORRESPONDING AUTHOR

Daoud Ali
Department of Zoology
College of Science
King Saud University Box 2455
Riyadh 11451, Saudi Arabia

e-mail: aalidaoud@ksu.edu.sa